Nonlinear MPC for Feedback-Interconnected Systems: a Suboptimal and Reduced-Order Model Approach

Stefano Di Gregorio, Guido Carnevale and Giuseppe Notarstefano

Abstract

In this paper, we propose a suboptimal and reduced-order Model Predictive Control (MPC) architecture for discrete-time feedback-interconnected systems. The numerical MPC solver: (i) acts suboptimally, performing only a finite number of optimization iterations at each sampling instant, and (ii) relies only on a reduced-order model that neglects part of the system dynamics, either due to unmodeled effects or the presence of a low-level compensator. We prove that the closed-loop system resulting from the interconnection of the suboptimal and reduced-order MPC optimizer with the full-order plant has a globally exponentially stable equilibrium point. Specifically, we employ timescale separation arguments to characterize the interaction between the components of the feedback-interconnected system. The analysis relies on an appropriately tuned timescale parameter accounting for how fast the system dynamics are sampled. The theoretical results are validated through numerical simulations on a mechatronic system consisting of a pendulum actuated by a DC motor.

I. INTRODUCTION

Model Predictive Control (MPC) is receiving increasing attention in both academia and industry as a powerful control technique for dynamical systems, see, e.g., [1]–[3] for a comprehensive overview of its theoretical and practical aspects.

The main drawback of MPC schemes lies in their computational complexity, which stems from the need to solve an optimal control problem online at each sampling instant. Consequently, a central challenge in current MPC research is to mitigate this limitation. In this context, we focus on two strategies that are widely adopted in both theoretical studies and practical implementations: (i) model order reduction, and (ii) suboptimal control approaches. When dealing with complex systems characterized by hierarchical structures or multiple interconnected subsystems, the computational complexity of MPC can become prohibitive. In such cases, reduced-order models can be employed to simplify the optimization problem while still capturing the essential dynamics of the system. In this spirit, the works [4]–[6] propose multi-rate control architectures, in which high-level routines based on MPC operate on reduced-order models and provide setpoints to low-level controllers acting on the full-order ones. This paradigm, which is very common in robotic applications, has been formalized in the tutorial work [7]. In [8], the authors guarantee the stability of the full closed-loop system despite the use of a reduced model in the MPC optimizer. A reduced-order MPC scheme is presented in [9], where stability and constraint satisfaction are proven while explicitly accounting for model reduction errors, whose bounds can be computed, e.g., as in [10]. In [11], Galerkin projection methods are employed to operate on a low-dimensional surrogate model. The authors of [12] present a robust MPC framework for two-time-scale linear systems, where only a reduced-order model neglecting the fast dynamics is used in the MPC optimizer.

Suboptimal MPC schemes have received considerable attention in the recent literature as a means to reduce the computational burden associated with standard MPC approaches. The main idea behind suboptimal MPC is to iteratively compute an approximate solution to the optimal control problem, rather than solving it exactly at each sampling instant. See, e.g., [13], [14] for an overview of suboptimal MPC schemes applied to nonlinear systems. The stability properties of suboptimal MPC have been investigated in [15]–[17]. In [18], the authors study the finite-time behavior of suboptimal linear MPC and provide insights into the trade-offs between computational efficiency and control performance. This work has been extended in [19] to nonlinear systems. In [20], a suboptimal MPC scheme is proposed with theoretical guarantees on closed-loop stability obtained by deriving an upper bound on the sampling time. More recently, [21] establishes the existence of a sampling-time bound under which the closed-loop system achieves exponential stability.

The main contribution of this paper lies in the design of an MPC architecture that combines suboptimal optimization and model reduction to reduce computational complexity. Specifically, we focus on nonlinear systems characterized by the feedback interconnection between a main target dynamics, that we aim to optimally control, and a faster extra dynamics (e.g., unmodeled dynamics or a low-level compensator). Inspired by [20] and [21], we interpret the small parameter enabling the timescale separation as the sampling time of the original continuous-time dynamics. Within this framework, we establish exponential stability of the equilibrium point of the closed-loop system resulting from the interconnection of the suboptimal and reduced-order MPC optimizer with the full-order plant.

The paper is organized as follows. In Section II, we present the problem setup. In Section III, we describe the proposed suboptimal and reduced-order MPC algorithm and state the stability properties of the closed-loop system. In Section IV, we provide the theoretical analysis. Finally, in Section V, we validate the theoretical results through numerical simulations.

The authors are with the Department of Electrical, Electronic and Information Engineering, University of Bologna, 40136, Bologna, Italy (e-mail: {stefano.digregorio, guido.carnevale, giuseppe.notarstefano}@unibo.it).

Notation: The symbols $\mathbb{R}$ and $\mathbb{N}$ denote the set of real and natural numbers, respectively. The symbol $\mathbb{R}_+$ denotes the set of positive real numbers. The symbol I_n denotes the identity matrix of dimension n. The symbol $0_{n \times m}$ denotes the zero matrix of dimension $n \times m$. The symbol $\| \cdot \|$ denotes the Euclidean norm. The symbol $\mathrm{diag}(d_1, \ldots, d_N)$ denotes the block-diagonal matrix with blocks $d_1, \ldots, d_N$ on the main diagonal. The symbol $\mathrm{col}(v_1, \ldots, v_N)$ denotes the vertical concatenation of the vectors $v_1, \ldots, v_N$.

II. SCENARIO DESCRIPTION

In this section, we describe the class of systems we consider in this work. In particular, we focus on discrete-time systems described by feedback-interconnected dynamics in the form

$$x_{t+1} = f(x_t, \xi_t, u_t, \delta) \tag{1a}$$
$$\xi_{t+1} = g(\xi_t, x_t, u_t, \delta), \tag{1b}$$

where $x_t \in \mathbf{X} \subseteq \mathbb{R}^n$ is the target state, $\xi_t \in \mathbf{\Xi} \subseteq \mathbb{R}^p$ is the extra dynamics state, $f : \mathbf{X} \times \mathbf{\Xi} \times \mathbf{U} \times \mathbb{R}_+ \to \mathbf{X}$ and $g : \mathbf{\Xi} \times \mathbf{X} \times \mathbf{U} \times \mathbb{R}_+ \to \mathbf{\Xi}$ denote the target and extra dynamics, respectively, $u_t \in \mathbf{U} \subseteq \mathbb{R}^m$ is the control input, and $\delta > 0$ is a parameter that allows to arbitrarily modulate the relative speed between the target state x_t and the extra dynamics state ξ_t. We formally characterize this property as follows.

Assumption 1: There exists $\bar{\delta}_1, L_f > 0$ such that, for all $\delta \in (0, \bar{\delta}_1)$, it holds

$$\|f(x, \xi, u, \delta) - f(x, \xi', u', \delta)\| \le \delta L_f \left(\|\xi - \xi'\| + \|u - u'\| \right),$$

for all $x \in \mathbf{X}$, $\xi, \xi' \in \mathbf{\Xi}$, and $u, u' \in \mathbf{U}$. Moreover, there exists $L_g > 0$ such that, for all $\delta \in (0, \bar{\delta}_1)$, it holds

$$\|g(\xi, x, u, \delta) - g(\xi', x', u', \delta)\| \le L_g \|\xi - \xi'\| + L_g \|x - x'\|$$
$$+ L_g \|u - u'\|,$$

for all $\xi, \xi' \in \mathbf{\Xi}$, $x, x' \in \mathbf{X}$, $u, u' \in \mathbf{U}$. ∎

The modeling framework in (1) can arise, e.g., from a discretization of a continuous-time system in which a subsystem evolves faster than the other subsystem (thanks, e.g., to a proper design of a low-level controller). Further, as we formalize in the following assumption, we consider the case in which the extra dynamics (1b) has equilibria parametrized in (x, u) and that these equilibria are globally exponentially stable, uniformly in (x, u).

Assumption 2: There exists a L_ξ-Lipschitz continuous function $\xi_{\mathrm{eq}} : \mathbf{X} \times \mathbf{U} \to \mathbf{\Xi}$ such that

$$g(\xi_{\mathrm{eq}}(x, u), x, u, \delta) = \xi_{\mathrm{eq}}(x, u), \tag{2}$$

for all $x \in \mathbf{X}$, $u \in \mathbf{U}$, and $\delta > 0$. Moreover, there exists a continuous function $U : \mathbf{\Xi} \to \mathbb{R}$ and $\bar{\delta}_2 > 0$ such that, for all $\delta \in (0, \bar{\delta}_2)$, it holds

$$a_1\|\tilde{\xi}\|^2 \le U(\tilde{\xi}) \le a_2\|\tilde{\xi}\|^2 \tag{3a}$$
$$U\big(g(\tilde{\xi} + \xi_{\mathrm{eq}}(x, u), x, u, \delta) - \xi_{\mathrm{eq}}(x, u)\big) - U(\tilde{\xi}) \le -a_3\|\tilde{\xi}\|^2 \tag{3b}$$
$$U(\tilde{\xi}) - U(\tilde{\xi}') \le a_4\|\tilde{\xi} - \tilde{\xi}'\|(\|\tilde{\xi}\| + \|\tilde{\xi}'\|), \tag{3c}$$

for all $\tilde{\xi}, \tilde{\xi}' \in \mathbf{\Xi}$, $x \in \mathbf{X}$, $u \in \mathbf{U}$ and some constants $a_1, a_2, a_3, a_4 > 0$. ∎

The practical intuition behind this assumption is that, in the ideal case in which x and u are fixed, the fast state ξ converges rapidly to a corresponding steady-state configuration $\xi_{\mathrm{eq}}(x, u)$. We provide in the following a practical example satisfying Assumptions 1 and 2.

Example 1: We consider a pendulum actuated by an electric motor whose continuous-time dynamics reads as

$$\dot{\theta}(t) = \omega(t) \tag{4a}$$
$$\dot{\omega}(t) = -\frac{\beta}{J}\omega(t) - \frac{mgl}{J}\sin\big(\theta(t)\big) + \frac{1}{J}K_t I(t) \tag{4b}$$
$$L\dot{I}(t) = V(t) - RI(t) - K_e\omega(t), \tag{4c}$$

where $\theta(t) \in \mathbb{S}^1$, $\omega(t) \in \mathbb{R}$, $I(t) \in \mathbb{R}$, and $V(t) \in \mathbb{R}$ are the pendulum angle, the angular velocity, the armature current, and the applied armature voltage at time $t \in \mathbb{R}$, respectively. As for the other elements in (4), $m, l, J > 0$ are the pendulum mass, length and total inertia, $g, \beta > 0$ are the gravitational acceleration and viscous friction coefficients, while $R, L, K_e, K_t > 0$ are the motor resistance, armature inductance, back EMF constant, and torque constant, respectively. By introducing $\mathrm{x}(t) := \mathrm{col}(\theta(t), \omega(t)) \in \mathbb{S}^1 \times \mathbb{R}$, $\chi(t) := I(t) \in \mathbb{R}$, $\mathrm{u}(t) := V(t) \in \mathbb{R}$, we rewrite (4) as

$$\dot{\mathrm{x}}(t) = \begin{bmatrix} \mathrm{x}_2(t) \\ -\frac{\beta}{J}\mathrm{x}_2(t) - \frac{mgl}{J}\sin(\mathrm{x}_1(t)) + \frac{K_t}{J}\chi(t) \end{bmatrix} \tag{5a}$$
$$\dot{\chi}(t) = -\frac{1}{L}\left(R\chi(t) + K_e\mathrm{x}_2(t) - \mathrm{u}(t)\right). \tag{5b}$$

By adopting a Forward-Euler discretization with sampling time $\delta > 0$ and choosing the armature inductance scaled as $L = \tilde{L}\delta$ with $\tilde{L} > 0$, we get a discretized counterpart of (5) described as

$$x_{t+1} = x_t + \delta \begin{bmatrix} x_{2,t} \\ -\frac{\beta}{J}x_{2,t} - \frac{mgl}{J}\sin(x_{1,t}) + \frac{K_t}{J}\xi_t \end{bmatrix} \tag{6a}$$

$$\xi_{t+1} = \left(1 - \frac{R}{\tilde{L}}\right)\xi_t - \begin{bmatrix} 0 & \frac{K_e}{\tilde{L}} \end{bmatrix} x_t + \frac{1}{\tilde{L}}u_t, \tag{6b}$$

where $x_t \in \mathbb{S}^1 \times \mathbb{R}$, $\xi_t \in \mathbb{R}$, and $u_t \in \mathbb{R}$ are the discrete-time counterparts at iteration t of $\mathrm{x}(t)$, $\chi(t)$, and $\mathrm{u}(t)$, respectively. System (6) is an instance of the generic system (1) in which the explicit expressions of f and g are given by

$$f(x, \xi, u, \delta) = x + \delta \begin{bmatrix} x_2 \\ -\frac{\beta}{J}x_2 - \frac{mgl}{J}\sin(x_1) + \frac{K_t}{J}\xi \end{bmatrix} \tag{7a}$$

$$g(\xi, x, u) = \left(1 - \frac{R}{\tilde{L}}\right)\xi - \begin{bmatrix} 0 & \frac{K_e}{\tilde{L}} \end{bmatrix} x + \frac{1}{\tilde{L}}u. \tag{7b}$$

Indeed, by observing (7a), we can see that system (6) satisfies Assumption 1 with $L_f = K_t/J$ and $L_g = \max\{1 - R/\tilde{L}, K_e/\tilde{L}, 1/\tilde{L}\}$. Moreover, by observing (7b), we also note that subsystem (6b) admits an equilibrium function $\xi_{\mathrm{eq}} : \mathbb{S}^1 \times \mathbb{R} \times \mathbb{R} \to \mathbb{R}$ defined as

$$\xi_{\mathrm{eq}}(x, u) = \frac{1}{R}\left(-\begin{bmatrix} 0 & K_e \end{bmatrix} x + u\right), \tag{8}$$

which satisfies Assumption 2 with $L_\xi = \max\{1, K_e\}/R$. Further, for all $\tilde{L} > R/2$, the equilibrium $\xi_{\mathrm{eq}}(x, u)$ is globally exponentially stable uniformly in $(x, u) \in \mathbb{S}^1 \times \mathbb{R} \times \mathbb{R}$ and, thus, Assumption 2 is satisfied.

III. SUBOPTIMAL AND REDUCED-ORDER MPC: STRATEGY DESCRIPTION AND STABILITY GUARANTEES

In this section, we introduce the proposed Suboptimal and Reduced-Order MPC strategy and provide the corresponding stability guarantees for the resulting closed-loop system.

A. MPC Strategy Description

By exploiting the system structure outlined in Section II, we design an MPC strategy that operates on a reduced-order model of system (1). Specifically, we approximate the full dynamics by a reduced dynamics map $f_R : \mathbf{X} \times \mathbf{U} \times \mathbb{R}_+ \to \mathbf{X}$ that captures the target subsystem f evaluated on the extra dynamics manifold $\xi = \xi_{\mathrm{eq}}(x, u)$, namely

$$f_R(x, u, \delta) := f(x, \xi_{\mathrm{eq}}(x, u), u, \delta). \tag{9}$$

The control input u_t is iteratively computed through a suboptimal MPC scheme applied to the reduced system, thereby adhering to and further reinforcing the rationale of computational efficiency motivating the use of f_R. In detail, given a time horizon $T \in \mathbb{N}$, at each iteration $t \in \mathbb{N}$, we consider the finite-horizon optimal control problem

$$\begin{aligned} \min_{\{u_\tau\}_{\tau=0}^{T-1}} \quad & \sum_{\tau=0}^{T-1} \ell(x_\tau, u_\tau) + \ell_T(x_T) \\ \text{s.t.} \quad & x_0 = x_t \\ & x_{\tau+1} = f_R(x_\tau, u_\tau, \delta), \quad \tau = 0, \dots, T-1 \\ & u_\tau \in \mathcal{U}, \quad x_{\tau+1} \in \mathcal{X}, \quad \tau = 0, \dots, T-1 \\ & x_T \in \mathcal{X}_f, \end{aligned} \tag{10}$$

where $\ell : \mathbf{X} \times \mathbf{U} \to \mathbb{R}_+$ is the stage cost, $\ell_T : \mathbf{X} \to \mathbb{R}_+$ is the terminal cost, $\mathcal{U} \subseteq \mathbf{U}$ is the input constraint set, $\mathcal{X} \subseteq \mathbf{X}$ is the state constraint set, and $\mathcal{X}_f \subseteq \mathbf{X}$ is the terminal constraint set. Problem (10) is addressed suboptimally. More in detail, we consider an optimizer dynamics of the form

$$z_{t+1} = \mathcal{T}(z_t, x_t) \tag{11a}$$

$$u_t = \Pi(z_t), \tag{11b}$$

where $z_t \in \mathbf{Z} \subseteq \mathbb{R}^{Tm}$ is the optimizer state, $\mathcal{T} : \mathbf{Z} \times \mathbf{X} \to \mathbf{Z}$ is the optimization algorithm, and $T \in \mathbb{N}$ is the prediction horizon. As customary in MPC schemes, only the first element of the z_t sequence is applied to the plant as control input, hence the projection map $\Pi : \mathbf{Z} \to \mathbf{U}$ in (11) reads as

$$\Pi(z) := \begin{bmatrix} I_m & 0_{m \times (T-1)m} \end{bmatrix} z. \tag{12}$$

In the following, some assumptions on the optimization algorithm are provided. By denoting with $z_\star(x)$ the unique solution of the problem (10) at given initial conditions x, we assume as follows that $z_\star(x)$ is a globally exponentially stable equilibrium point of the optimizer dynamics (11).

Assumption 3: For all $x \in \mathbf{X}$, it holds

$$z_\star(x) = \mathcal{T}(z_\star(x), x). \tag{13}$$

Moreover, there exists a continuous function $\mathcal{L} : \mathbf{Z} \to \mathbb{R}_+$ such that

$$b_1 \|z - z_\star(x)\|^2 \leq \mathcal{L}(z) \leq b_2 \|z - z_\star(x)\|^2 \tag{14a}$$

$$\mathcal{L}(\mathcal{T}(z,x)) - \mathcal{L}(z) \leq -b_3 \|z - z_\star(x)\|^2 \tag{14b}$$

$$\mathcal{L}(z) - \mathcal{L}(z') \leq b_4 \|z - z'\| \left(\|z - z_\star(x)\| + \|z' - z_\star(x)\|\right), \tag{14c}$$

for all $z, z' \in \mathbf{Z}$, $x \in \mathbf{X}$, and some $b_1, b_2, b_3, b_4 > 0$. Further, the functions $\mathcal{T}$ and $z_\star$ are $L_{\mathcal{T}}$- and $L_{z_\star}$-Lipschitz continuous, respectively, for some $L_{\mathcal{T}}, L_{z_\star} > 0$. ∎

As is standard in MPC (see, e.g., [3]), we assume that the optimal solution to (10) yields an exponentially stable equilibrium $x_\star \in \mathbf{X}$ for the reduced system.

Assumption 4: There exists a continuous function $W : \mathbf{X} \to \mathbb{R}$ and $\bar{\delta}_3 > 0$ such that for all $\delta \in (0, \bar{\delta}_3)$

$$c_1 \|x - x_\star\|^2 \leq W(x) \leq c_2 \|x - x_\star\|^2 \tag{15a}$$

$$W(f_R(x, \Pi(z_\star(x)), \delta)) - W(x) \leq -\delta c_3 \|x - x_\star\|^2 \tag{15b}$$

$$W(x) - W(x') \leq c_4 \|x - x'\| \left(\|x\| + \|x'\|\right), \tag{15c}$$

for all $x, x' \in \mathbf{X}$ and some $c_1, c_2, c_3, c_4 > 0$. ∎

B. Closed-Loop System: Stability Guarantees

The closed-loop system is thus described by the interconnection of the plant (1) and the optimizer (11), namely

$$x_{t+1} = f(x_t, \xi_t, \Pi(z_t), \delta) \tag{16a}$$

$$\xi_{t+1} = g(\xi_t, x_t, \Pi(z_t), \delta) \tag{16b}$$

$$z_{t+1} = \mathcal{T}(z_t, x_t), \tag{16c}$$

Fig. 1 shows a schematic representation of the closed-loop system in the pendulum-motor setup in Example 1.
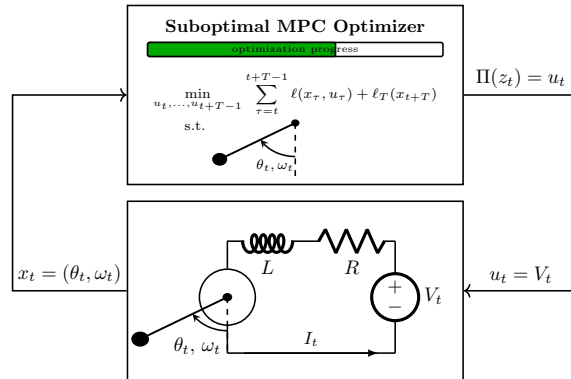

Fig. 1. Block diagram representation of the closed-loop system resulting from the interconnection of the full plant dynamics (1) and the reduced-order suboptimal MPC (11) for the pendulum-motor setup (cf. Example 1).

The stability properties of the closed-loop system (16) are formalized as follows.

Theorem 1: Consider the closed-loop system (16) and let Assumptions 1, 2, 3, and 4 hold. Then, there exists $\bar{\delta} \in (0, \min\{\bar{\delta}_1, \bar{\delta}_2, \bar{\delta}_3\})$ such that, for all $\delta \in (0, \bar{\delta})$, the point $(x_\star, \xi_{\mathrm{eq}}(x_\star, \Pi(z_\star(x_\star))), z_\star(x_\star))$ is a globally exponentially stable equilibrium of system (16). ∎

The proof of Theorem 1 is provided in Section IV-C after the preparatory analysis developed in Section IV.

IV. THEORETICAL ANALYSIS

In this section, we analyze the closed-loop system arising from the interconnection of the plant dynamics (1) and the optimizer one (11) to prove Theorem 1. More in detail, we interpret this closed-loop system as a two-time-scale system in which the fast subsystem includes both the plant extra dynamics (1b) and the optimizer dynamics (11), while the slow part includes only the plant target dynamics (1a). This feedback interconnection is graphically depicted in Fig. 2.
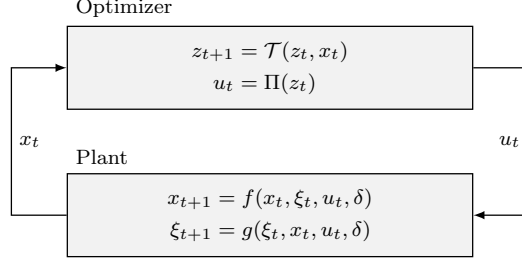

Fig. 2.   Block diagram representation of the interconnected system.

Hence, as customary in two-time-scale system analysis, we study (i) the fast subsystem in the ideal case in which the slow state x_t is fixed (cf. Section IV-B) and, conversely, (ii) the slow one in the ideal case in which the fast state (ξ_t, z_t) lies in its equilibrium manifold (cf. Section IV-B). Finally, in Section IV-C we combine the results obtained in this preparatory phase to prove Theorem 1.

A. Boundary-Layer System Analysis

Here, we focus on the boundary-layer system, i.e., the subsystem obtained by considering an arbitrarily fixed slow state $x_t = x$ for all $t \in \mathbb{N}$ in the fast subsystem (16b)-(16c). A graphical representation of this system is shown in Fig. 3.
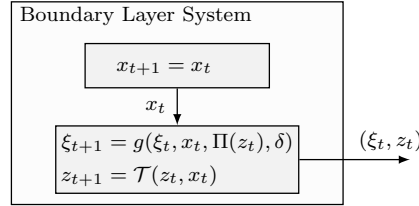

Fig. 3.   Block diagram representation of the boundary layer system.

Hence, by observing (16b)-(16c) and introducing the error coordinates $\mathrm{col}(\tilde{\xi}_t, \tilde{z}_t) := \mathrm{col}(\xi_t - \xi_{\mathrm{eq}}(x, \Pi(z_t)), z_t - z_\star(x))$, the boundary-layer system reads as

$$\tilde{\xi}_{t+1} = g(\tilde{\xi}_t + \xi_{\mathrm{eq}}(x, \Pi(\tilde{z}_t + z_\star(x))), x, \Pi(\tilde{z}_t + z_\star(x)), \delta)$$
$$- \xi_{\mathrm{eq}}(x, \Pi(\mathcal{T}(\tilde{z}_t + z_\star(x), x))) \tag{17a}$$
$$\tilde{z}_{t+1} = \mathcal{T}(\tilde{z}_t + z_\star(x), x) - z_\star(x). \tag{17b}$$

For the sake of compactness, let $\tilde{g} : \Xi \times \mathbf{X} \times \mathbf{Z} \times \mathbb{R}_+ \to \Xi$, $\tilde{\mathcal{T}} : \mathbf{Z} \times \mathbf{X} \to \mathbf{Z}$, and $\Delta\xi_{\mathrm{eq}} : \mathbf{X} \times \mathbf{Z} \to \Xi$ be defined as

$$\tilde{g}(\tilde{\xi}, x, \Pi(\tilde{z}), \delta) := g(\tilde{\xi} + \xi_{\mathrm{eq}}(x, \Pi(\tilde{z})), x, \Pi(\tilde{z}), \delta)$$
$$- \xi_{\mathrm{eq}}(x, \Pi(\tilde{z})) \tag{18a}$$
$$\tilde{\mathcal{T}}(\tilde{z}, x) := \mathcal{T}(\tilde{z} + z_\star(x), x) - z_\star(x) \tag{18b}$$
$$\Delta\xi_{\mathrm{eq}}(x, \tilde{z}, \tilde{z}') := \xi_{\mathrm{eq}}(x, \Pi(\tilde{z} + z_\star(x)))$$
$$- \xi_{\mathrm{eq}}(x, \Pi(\tilde{z}' + z_\star(x))), \tag{18c}$$

which allow us to compactly rewrite (19) as

$$\tilde{\xi}_{t+1} = \tilde{g}(\tilde{\xi}_t, x, \Pi(\tilde{z}_t + z_\star(x)), \delta) + \Delta\xi_{\mathrm{eq}}(x, \tilde{z}_{t+1}, \tilde{z}_t) \tag{19a}$$
$$\tilde{z}_{t+1} = \tilde{\mathcal{T}}(\tilde{z}_t, x). \tag{19b}$$

The following lemma ensures global exponential stability of the origin for the boundary-layer system (19).

Lemma 1: There exists a continuous function $\mathcal{U} : \Xi \times \mathbf{Z} \to \mathbb{R}$ such that, for all $\delta \in (0, \min\{\bar{\delta}_1, \bar{\delta}_2\})$, it holds

$$d_1(\|\tilde{\xi}\|^2 + \|\tilde{z}\|^2) \leq \mathcal{U}(\tilde{\xi}, \tilde{z}) \leq d_2(\|\tilde{\xi}\|^2 + \|\tilde{z}\|^2) \tag{20a}$$

$$\mathcal{U}(\tilde{\xi}_+, \tilde{z}_+) - \mathcal{U}(\tilde{\xi}, \tilde{z}) \leq -d_3(\|\tilde{\xi}\|^2 + \|\tilde{z}\|^2) \tag{20b}$$

$$\mathcal{U}(\tilde{\xi}, \tilde{z}) - \mathcal{U}(\tilde{\xi}', \tilde{z}') \leq d_4 \left\| \mathrm{col}(\tilde{\xi}, \tilde{z}) - \mathrm{col}(\tilde{\xi}', \tilde{z}') \right\| \tag{20c}$$

$$\times \left(\| \mathrm{col}(\tilde{\xi}, \tilde{z}) \| + \| \mathrm{col}(\tilde{\xi}', \tilde{z}') \| \right),$$

for all $\tilde{\xi} \in \Xi$, $\tilde{z} \in \mathbf{Z}$, $x \in \mathbf{X}$, and some constants $d_1, d_2, d_3, d_4 > 0$, where $\tilde{\xi}_+ := \tilde{g}(\tilde{\xi}, x, \Pi(\tilde{z} + z_\star(x)), \delta) + \Delta \xi_{\mathrm{eq}}(x, \tilde{z}, \tilde{\mathcal{T}}(\tilde{z}, x))$ and $\tilde{z}_+ := \tilde{\mathcal{T}}(\tilde{z}, x)$. ∎

The proof of Lemma 1 is provided in Appendix VI-B.

B. Reduced System Analysis

As graphically depicted in Fig. 4, the reduced system corresponds to the slow subsystem (16a) studied by considering the fast state (ξ_t, z_t) in its equilibrium manifold, i.e., $\xi_t = \xi_{\mathrm{eq}}(x_t, \Pi(z_t))$ and $z_t = z_\star(x_t)$ for all $t \in \mathbb{N}$.

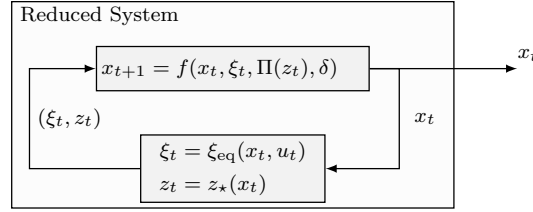
Fig. 4.   Block diagram representation of the reduced system.

Then, by definition of f_R in (9), the reduced system reads

$$x_{t+1} = f_R(x_t, \Pi(z_\star(x_t)), \delta). \tag{21}$$

Therefore, the reduced system convergence properties directly follow from Assumption 4.

C. Proof of Theorem 1

The proof of Theorem 1 consists in merging the results achieved in Sections IV-A and IV-B to invoke the generic timescale separation result formalized in Theorem 2 (cf. Appendix VI-A). In order to apply this result, we need to check that its requirements are satisfied. First, by observing the requirement in (27), we need a Lyapunov function proving the exponential stability of the origin for the boundary-layer system (19) and we achieve it by Lemma 1. Second, by observing the requirement in (28), we need a Lyapunov function proving the exponential stability of $x_\star$ for our reduced system (21) and we achieve it by Assumption 4. Finally, we need the Lipschitz continuity of the equilibrium function $\mathrm{col}(\xi_{\mathrm{eq}}(x, \Pi z_\star(x)), z_\star(x))$ and the fast system dynamics as well as the conditions (23a) and (29) on the slow dynamics. These conditions are satisfied by Assumptions 1, 2, and 3. Thus, we guarantee that $(x_\star, \xi_{\mathrm{eq}}(x_\star, \Pi z_\star(x_\star)), z_\star(x_\star))$ is a globally exponentially stable equilibrium of system (16) by invoking Theorem 2 and the proof concludes.

V. NUMERICAL SIMULATIONS

In this section, we present numerical simulations to validate the proposed Suboptimal and Reduced-Order MPC control strategy. In particular, we consider the actuated pendulum introduced in Example 1, whose physical parameters values are reported in Table I.

TABLE I

PHYSICAL PARAMETERS OF THE ACTUATED PENDULUM

Parameter	Value
l	1.0[m]
m	0.5[Kg]
β	0.5[N m s/rad]
J	0.5[Kg m^2]
K_t	0.4[N m/A]
K_e	0.4[V s/rad]
R	0.6[Ω]
L	$\tilde{L}\delta$ [H]
$\tilde{L}$	1.0 [H]

Consistently with the theoretical setting, the optimizer is only aware of the reduced-order model obtained by considering (6a) in the case in which the armature current ξ_t lies in its equilibrium manifold (8). Namely, in this scenario, the reduced dynamics map (9) explicitly reads as

$$f_R(x, u, \delta) := \begin{bmatrix} x_1 + \delta x_2 \\ x_2 + \delta\left(-\frac{g}{l}\sin(x_1) - \frac{\beta}{ml^2}x_2 + \frac{K_t}{ml^2}\frac{R}{K_e}u\right) \end{bmatrix}.$$

We consider a finite-horizon optimal control problem (10) with cost functions given by

$$\ell(x, u) := x^\top Q x + u^\top R u, \quad \ell_T(x) := x^\top Q_f x,$$

with $Q = Q_f = \operatorname{diag}(100, 0.1)$, $R = 0.01$ and the prediction horizon $T = T_s\delta$ with $T_s = 0.5$s. The input is subject to a saturation constraint $\mathcal{U} = \{u \in \mathbb{R} \mid |u| \leq 24\}$ and the MPC problem is addressed through a suboptimal scheme. We compare the proposed approach (*Suboptimal and Red. Order*), where the MPC optimizer relies on a reduced-order prediction model while interacting with the full-order plant, with two benchmark settings: *Suboptimal and Full-Order* and *Optimal and Full-Order*, where the MPC operates suboptimally and optimally, respectively. In both these benchmarks, the plant dynamics is reduced and, thus, coincides with the reduced-order prediction model, allowing the optimizer to fully capture the system behavior. These strategies are compared in three scenarios in which different δ are used. As predicted by Theorem 1, Fig. 5 shows that the closed-loop system exhibits exponential convergence towards the desired equilibrium configuration when a sufficiently small $\delta = 0.01s$ is used. Fig. 6 highlights the importance of timescale separation. Indeed, for a larger value of δ ($\delta = 0.1s$), although the suboptimal MPC optimizer operating on the full-order model still provides acceptable closed-loop behavior, the one operating on the reduced-order model exhibits a performance degradation. Finally, Fig. 7 further confirms the need for timescale separation. Indeed, in this case with $\delta = 0.2s$, only the optimal MPC optimizer operating on the full-order model guarantees good closed-loop performance, while both the suboptimal MPC optimizers (operating on the full-order and reduced-order models) lead to a significant performance degradation.
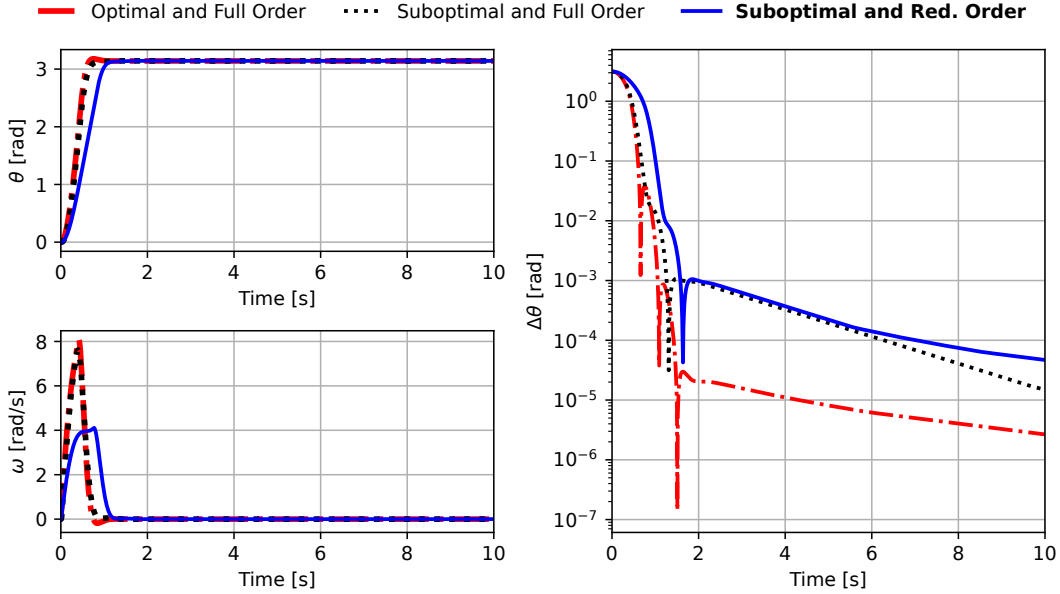

Fig. 5. Closed-loop trajectories of the target states θ and ω (left) and angular position error in semilog scale (right) for $\delta = 0.01$ s.

VI. CONCLUSIONS

We proposed a suboptimal and reduced-order MPC scheme for discrete-time interconnected systems. The approach relies on a reduced-order model that omits part of the plant dynamics, enabling a lighter computational burden while maintaining formal closed-loop stability guarantees. In particular, we showed that closed-loop stability can be preserved by properly tuning a timescale parameter. Numerical simulations on an actuated pendulum confirmed the effectiveness of our approach.

APPENDIX

A. Global Exponential Stability of Two-Time-Scales Systems

The following result provides sufficient conditions for the global exponential stability of two-time-scale discrete-time systems. It is a slight extension of [22, Thm. II.5], since here we allow for generic slow dynamics in place of the specific form $x_{t+1} = x_t + \delta f(x_t, w_t)$ considered there.
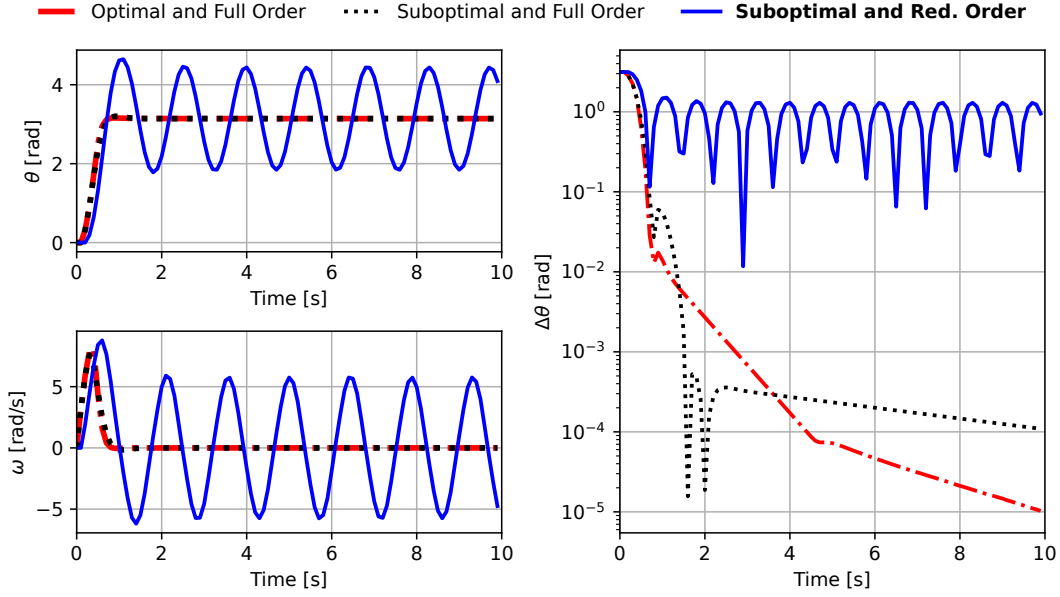
Fig. 6. Closed-loop trajectories of the target states θ and ω (left) and angular position error in semilog scale (right) for $\delta = 0.1$ s.
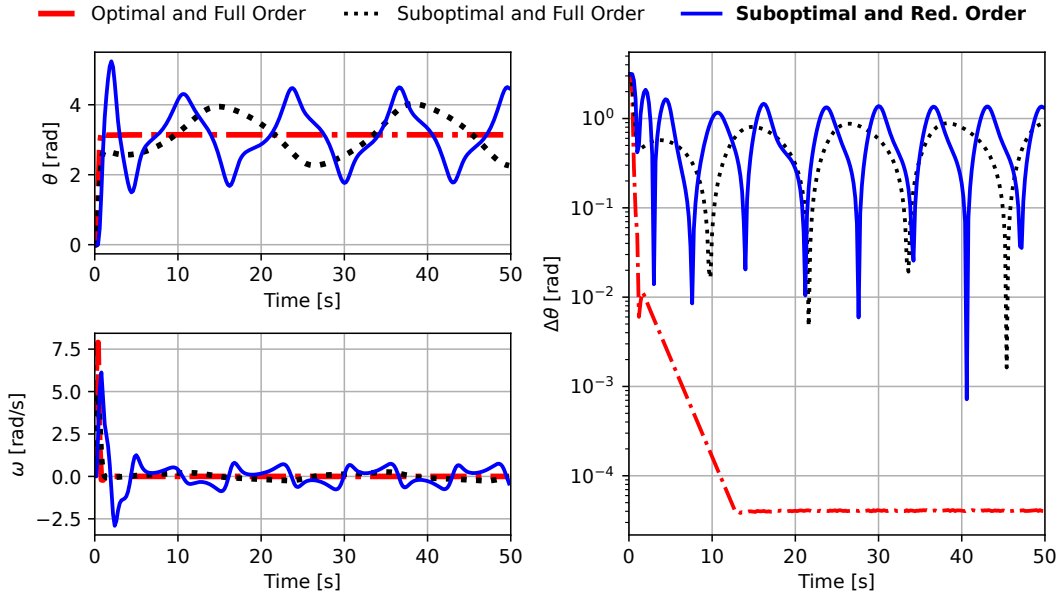

Fig. 7. Closed-loop trajectories of the target states θ and ω (left) and angular position error in semilog scale (right) for $\delta = 0.2$ s.

Theorem 2: Consider the system

$$x_{t+1} = f(x_t, w_t, \delta) \tag{22a}$$

$$w_{t+1} = G(w_t, x_t, \delta), \tag{22b}$$

with $x_t \in \mathbf{X} \subseteq \mathbb{R}^n$, $w_t \in \mathbf{\Xi} \subseteq \mathbb{R}^m$, $f : \mathbf{X} \times \mathbf{\Xi} \times \mathbb{R} \to \mathbf{X}$, $G : \mathbf{\Xi} \times \mathbf{X} \times \mathbb{R} \to \mathbf{\Xi}$, $\delta > 0$. Assume that there exist $L_f, L_g, \bar{\delta}_1 > 0$ such that for all $\delta \in (0, \bar{\delta}_1)$, it holds

$$\|f(x, w, \delta) - f(x', w', \delta)\| \le L_f \|x - x'\| + \delta L_f \|w - w'\| \tag{23a}$$

$$\|G(w, x, \delta) - G(w', x', \delta)\| \le L_g(\|w - w'\| + \|x - x'\|) \tag{23b}$$

for all $x, x' \in \mathbf{X}$, $w, w' \in \mathbf{\Xi}$. Assume that there exists an L_h-Lipschitz continuous function $h : \mathbf{X} \to \mathbf{\Xi}$ such that

$$h(x) = G(h(x), x, \delta), \tag{24}$$

for all $x \in \mathbf{X}$. Assume also that there exists $x_\star \in \mathbf{X}$ such that $x_\star = f(x_\star, h(x_\star), \delta)$, for all $\delta > 0$. Then, let

$$x_{t+1} = f(x_t, h(x_t), \delta) \tag{25}$$

be the *reduced system* and

$$\psi_{t+1} = G(\psi_t + h(x), x, \delta) - h(x) \tag{26}$$

be the *boundary layer system* with $\psi_t \in \Xi$.

Assume that there exists a continuous function $U : \Xi \to \mathbb{R}$ such that, for all $\delta \in (0, \bar{\delta}_2)$, there exist $b_1, b_2, b_3, b_4 > 0$ such that for all $\psi, \psi_1, \psi_2 \in \Xi$, $x \in \mathbf{X}$, it holds

$$b_1 \|\psi\|^2 \le U(\psi) \le b_2 \|\psi\|^2 \tag{27a}$$

$$U(G(\psi + h(x), x, \delta) - h(x)) - U(\psi) \le -b_3 \|\psi\|^2 \tag{27b}$$

$$U(\psi_1) - U(\psi_2) \le b_4 \|\psi_1 - \psi_2\| (\|\psi_1\| + \|\psi_2\|). \tag{27c}$$

Assume also that there exists a continuous function $W : \mathbf{X} \to \mathbb{R}$ and $\bar{\delta}_3 > 0$ such that, for all $\delta \in (0, \bar{\delta}_3)$, it holds

$$c_1 \|x - x_\star\|^2 \le W(x) \le c_2 \|x - x_\star\|^2 \tag{28a}$$

$$W(f(x, h(x), \delta)) - W(x) \le -\delta c_3 \|x - x_\star\|^2 \tag{28b}$$

$$W(x_1) - W(x_2) \le c_4 \|x_1 - x_2\| (\|x_1 - x_\star\| + \|x_2 - x_\star\|), \tag{28c}$$

for all $x, x_1, x_2, x_3 \in \mathbf{X}$ and some $c_1, c_2, c_3, c_4 > 0$. Finally, assume that, for all $x \in \mathbf{X}$ and $\delta > 0$, it holds

$$\|f(x, h(x), \delta) - x\| \le \delta L_f \|x - x_\star\|. \tag{29}$$

Then, there exist $\bar{\delta} \in (0, \min\{\bar{\delta}_1, \bar{\delta}_2, \bar{\delta}_3\})$, $a_1 > 0$, and $a_2 > 0$ such that, for all $\delta \in (0, \bar{\delta})$, it holds

$$\left\| \begin{bmatrix} x_t - x_\star \\ w_t - h(x_t) \end{bmatrix} \right\| \le a_1 \left\| \begin{bmatrix} x^0 - x_\star \\ w^0 - h(x^0) \end{bmatrix} \right\| e^{-a_2 t},$$

for all $(x^0, w^0) \in \mathbf{X} \times \Xi$.

Proof: Let us introduce $\tilde{w}_t := w_t - h(x_t)$ and accordingly rewrite system (22) as

$$x_{t+1} = f(x_t, \tilde{w}_t + h(x_t), \delta) \tag{30a}$$

$$\tilde{w}_{t+1} = G(\tilde{w}_t + h(x_t), x_t, \delta) - h(x_{t+1}). \tag{30b}$$

Select W as in (28). By evaluating $\Delta W(x) := W(f(x, \tilde{w} + h(x), \delta)) - W(x)$ along the trajectories of (30a), we obtain

$$\Delta W(x) = W(f(x, \tilde{w} + h(x), \delta)) - W(x)$$

$$\stackrel{(a)}{=} W(f(x, h(x), \delta)) - W(x)$$
$$\quad + W(f(x, \tilde{w} + h(x), \delta)) - W(f(x, h(x), \delta))$$

$$\stackrel{(b)}{\le} -\delta c_3 \|x - x_\star\|^2 + W(f(x, \tilde{w} + h(x), \delta))$$
$$\quad - W(f(x, h(x), \delta))$$

$$\stackrel{(c)}{\le} -\delta c_3 \|x - x_\star\|^2 + \delta c_4 L_f \|\tilde{w}\| \|f(x, h(x), \delta) - x_\star\|$$
$$\quad + \delta c_4 L_f \|\tilde{w}\| \|f(x, \tilde{w} + h(x), \delta) - x_\star\|, \tag{31}$$

where in (a) we add $\pm W(f(x, h(x), \delta))$, in (b) we use (28b) to bound the first two terms, in (c) we use (28c) and (23a). By using (23a), (29), and the triangle inequality, we note that

$$\|f(x, \tilde{w} + h(x), \delta) - x_\star\| \le (1 + \delta L_f) \|x - x_\star\| + \delta L_f \|\tilde{w}\|. \tag{32a}$$

$$\|f(x, h(x), \delta) - x_\star\| \le (1 + \delta L_f) \|x - x_\star\|. \tag{32b}$$

Using inequalities (32a) and (32b) we then bound (31) as

$$\Delta W(x) \le -\delta c_3 \|x - x_\star\|^2 + \delta^2 k_3 \|\tilde{w}\|^2$$
$$\quad + (\delta k_1 + \delta^2 k_2) \|\tilde{w}\| \|x - x_\star\|, \tag{33}$$

introducing $k_1 := 2c_4 L_f, k_2 := 2c_4 L_f^2, k_3 := c_4 L_f^2$. Now, let us introduce $\Delta h : \mathbf{X} \times \Xi \times \mathbb{R} \to \Xi$ defined as

$$\Delta h(x, \tilde{w}, \delta) := -h(f(x, \tilde{w} + h(x), \delta)) + h(x). \tag{34}$$

Then, we select U as in (27). By adding and subtracting $U(G(\tilde{w}_t+h(x_t)), x_t, \delta)-h(x_t))$ to $\Delta U(\tilde{w}) := U(G(\tilde{w}+h(x), x, \delta)-h(f(x, \tilde{w}+h(x), \delta))) - U(\tilde{w})$, we obtain

$$
\begin{aligned}
&\Delta U(\tilde{w}) - U(\tilde{w}) \\
&= U(G(\tilde{w}+h(x), x, \delta) - h(x)) - U(\tilde{w}) \\
&\quad - U(G(\tilde{w}+h(x), x, \delta) - h(x)) \\
&\quad + U(G(\tilde{w}+h(x), x, \delta) - h(f(x, \tilde{w}+h(x), \delta))) \\
&\overset{(a)}{\leq} -b_3 \|\tilde{w}\|^2 - U(G(\tilde{w}+h(x), x, \delta) - h(x)) \\
&\quad + U(G(\tilde{w}+h(x), x, \delta) - h(f(x, \tilde{w}+h(x), \delta))) \\
&\overset{(b)}{\leq} -b_3 \|\tilde{w}\|^2 + b_4 \|\Delta h(x, \tilde{w}, \delta)\| \\
&\quad\quad\quad \times \|G(\tilde{w}+h(x), x, \delta) - h(f(x, \tilde{w}+h(x), \delta))\| \\
&\quad + b_4 \|\Delta h(x, \tilde{w}, \delta)\| \|G(\tilde{w}+h(x), x, \delta) - h(x)\| \\
&\overset{(c)}{\leq} -b_3 \|\tilde{w}\|^2 + b_4 \|\Delta h(x, \tilde{w}, \delta)\|^2 \\
&\quad + 2b_4 \|\Delta h(x, \tilde{w}, \delta)\| \|G(\tilde{w}+h(x), x, \delta) - h(x)\|,
\end{aligned}
\tag{35}
$$

where in (a) we exploit (27b) to bound the first two terms, in (b) we use (27c) to bound the the difference of the last two terms, and in (c) we use the triangle inequality. By definition of Δh (cf. (34)) and Lipschitz continuity of h, we write

$$
\begin{aligned}
\|\Delta h(x, \tilde{w}, \delta)\| &\leq L_h \|f(x, \tilde{w}+h(x), \delta) - x\| \\
&\overset{(a)}{\leq} L_h \|f(x, h(x), \delta) - x\| \\
&\quad + L_h \|f(x, \tilde{w}+h(x), \delta) - f(x, h(x), \delta)\| \\
&\overset{(b)}{\leq} \delta L_h L_f \|x - x_\star\| + \delta L_h L_f \|\tilde{w}\|,
\end{aligned}
\tag{36}
$$

where in (a) we add and subtract $f(x, h(x), \delta)$ in the norm and apply the triangle inequality, while in (b) we apply (29) to bound the first term and (23a) to bound the second one. Moreover, since $G(h(x), x, \delta) = h(x)$ (cf. (24)), we obtain

$$
\begin{aligned}
&\|G(\tilde{w}+h(x), x, \delta) - h(x)\| \\
&= \|G(\tilde{w}+h(x), x, \delta) - G(h(x), x, \delta)\| \leq L_G \|\tilde{w}\|,
\end{aligned}
\tag{37}
$$

where the inequality is due to the Lipschitz continuity of G (cf. (23b)). Using inequalities (36) and (37), we then bound (35) as

$$
\begin{aligned}
\Delta U(\tilde{w}) &\leq -b_3 \|\tilde{w}\|^2 + 2\delta b_4 L_h L_G L_f \|\tilde{w}\|^2 \\
&\quad + 2\delta b_4 L_h L_G L_f \|x - x_\star\| \|\tilde{w}\| \\
&\quad + 2\delta^2 b_4 L_h^2 L_f^2 \|x - x_\star\| \|\tilde{w}\| + \delta^2 b_4 L_h^2 L_f^2 \|\tilde{w}\|^2 \\
&\quad + \delta^2 b_4 L_h^2 L_f^2 \|x - x_\star\|^2 \\
&\leq (-b_3 + \delta k_6 + \delta^2 k_7) \|\tilde{w}\|^2 + \delta^2 k_8 \|x - x_\star\|^2 \\
&\quad + (\delta k_4 + \delta^2 k_5) \|x - x_\star\| \|\tilde{w}\|,
\end{aligned}
\tag{38}
$$

where we introduce the constants

$$
\begin{aligned}
k_4 &:= 2b_4 L_h L_G L_f, & k_5 &:= 2b_4 L_h^2 L_f^2, \ k_6 := 2b_4 L_h L_G L_f, \\
k_7 &:= b_4 L_h^2 L_f^2, & k_8 &:= b_4 L_h^2 L_f^2.
\end{aligned}
$$

We pick the following Lyapunov candidate $V : \mathbf{X} \times \mathbf{\Xi} \to \mathbb{R}$:

$$
V(x, \tilde{w}) = W(x) + U(\tilde{w}).
$$

By evaluating the increment $\Delta V(x, \tilde{w}) := V(f(x, \tilde{w}+h(x), \delta), G(\tilde{w}+h(x), x, \delta) - h(f(x, \tilde{w}+h(x), \delta))) - V(x, \tilde{w}) = \Delta W(x) + \Delta U(\tilde{w})$ of V along the trajectories of system (30), we can use the results (33) and (38) to write

$$
\Delta V(x, \tilde{w}) \leq - \begin{bmatrix} \|x - x_\star\| \\ \|\tilde{w}\| \end{bmatrix}^\top Q(\delta) \begin{bmatrix} \|x - x_\star\| \\ \|\tilde{w}\| \end{bmatrix},
\tag{39}
$$

where we define the matrix $Q(\delta) = Q(\delta)^\top \in \mathbb{R}^2$ as

$$Q(\delta) := \begin{bmatrix} \delta c_3 - \delta^2 k_8 & q_{21}(\delta) \\ q_{21}(\delta) & b_3 - \delta k_6 - \delta^2(k_3 + k_7) \end{bmatrix},$$

with $q_{21}(\delta) := -\frac{1}{2}(\delta(k_1 + k_4) + \delta^2(k_2 + k_5))$. By Sylvester criterion, we know that $Q \succ 0$ if and only if

$$c_3 b_3 > p(\delta), \tag{40}$$

where the polynomial $p(\delta)$ is defined as

$$\begin{aligned} p(\delta) := {}& q_{21}(\delta)^2 + \delta^2 c_3 k_6 + \delta^2(\delta c_3(k_3 + k_7) + b_3 k_8) \\ & - \delta^3 k_6 k_8 - \delta^4 k_8(k_3 + k_7). \end{aligned} \tag{41}$$

Since p is a continuous function of δ and $\lim_{\delta \to 0} p(\delta) = 0$, there exists $\bar{\delta} \in (0, \min\{\bar{\delta}_1, \bar{\delta}_2, \bar{\delta}_3\})$ so that (40) is satisfied for any $\delta \in (0, \bar{\delta})$. Under this choice of δ and denoting by $q > 0$ the smallest eigenvalue of $Q(\delta)$, we bound (39) as

$$\Delta V(x, \tilde{w}) \leq -q \|x - x_\star\|^2 + \|\tilde{w}\|^2,$$

which allows us to conclude, in view of [23, Theorem 13.2], that $(x_\star, 0)$ is an exponentially stable equilibrium point for system (30). The conclusion of the theorem follows by considering the definition of exponentially stable equilibrium point and by reverting to the original coordinates (x, w). ∎

B. Proof of Lemma 1

The proof consists in combining the exponential stability properties of the fast dynamics (1b) stated in Assumption 2 with those of the optimizer dynamics (11) stated in Assumption 3, and in suitably handling the drift of the fast plant equilibrium $\xi_{\text{eq}}(x, \Pi(\tilde{z}_t + z_\star(x)))$ due to the variations of $\tilde{z}_t$. Purposely, let the function $\mathcal{U} : \Xi \times \mathbf{Z} \to \mathbb{R}$ be defined as

$$\mathcal{U}(\tilde{\xi}, \tilde{z}) := U(\tilde{\xi}) + \kappa \mathcal{L}(\tilde{z}), \tag{42}$$

where U and $\mathcal{L}$ are introduced in (3) (cf. Assumption 2) and (14) (cf. Assumption 3), respectively, while $\kappa > 0$ is a constant that we will set later. We note that (20a) and (20c) directly follow by combining (3a) with (14a) for the former and (3c) with (14c) for the latter. To prove (20b), we introduce a more compact notation by defining the shorthands

$$\tilde{\xi}_+ := \tilde{g}(\tilde{\xi}, x, \Pi(\tilde{z} + z_\star(x)), \delta) + \Delta \xi_{\text{eq}}(x, \tilde{z}_+, \tilde{z}) \tag{43a}$$

$$\tilde{z}_+ := \tilde{\mathcal{T}}(\tilde{z}, x), \quad \tilde{\xi}_+^{\text{nom}} := \tilde{g}(\tilde{\xi}, x, \Pi(\tilde{z} + z_\star(x)), \delta). \tag{43b}$$

With this notation at hand, the increment $\Delta \mathcal{U}(\tilde{\xi}, \tilde{z}) := \mathcal{U}(\tilde{\xi}_+, \tilde{z}_+) - \mathcal{U}(\tilde{\xi}, \tilde{z})$ of $\mathcal{U}$ (cf. (42)) along the trajectories of the boundary-layer system (19) reads as

$$\begin{aligned} \Delta \mathcal{U}(\tilde{\xi}, \tilde{z}) = {}& U(\tilde{\xi}_+) - U(\tilde{\xi}) + \kappa \left(\mathcal{L}(\tilde{z}_+) - \mathcal{L}(\tilde{z}) \right) \\ & \overset{(a)}{\leq} U(\tilde{\xi}_+) - U(\tilde{\xi}) - \kappa b_3 \|\tilde{z}\|^2 \\ & \overset{(b)}{=} U(\tilde{\xi}_+^{\text{nom}}) - U(\tilde{\xi}) - \kappa b_3 \|\tilde{z}\|^2 + U(\tilde{\xi}_+) - U(\tilde{\xi}_+^{\text{nom}}) \\ & \overset{(c)}{\leq} -a_3 \left\| \tilde{\xi} \right\|^2 - \kappa b_3 \|\tilde{z}\|^2 + U(\tilde{\xi}_+) - U(\tilde{\xi}_+^{\text{nom}}), \end{aligned} \tag{44}$$

where in (a) we apply (14b) (cf. Assumption 3), in (b) we add $\pm U(\tilde{\xi}_+^{\text{nom}})$, while in (c) we apply (3b). Now, we focus on the term $U(\tilde{\xi}_+) - U(\tilde{\xi}_+^{\text{nom}})$. By using the bound (3c) and the definitions of $\tilde{\xi}_+$ (cf. (43a)) and $\tilde{\xi}_+^{\text{nom}}$ (cf. (43b)), we get

$$\begin{aligned} & U(\tilde{\xi}_+) - U(\tilde{\xi}_+^{\text{nom}}) \\ & \leq a_4 \|\Delta \xi_{\text{eq}}(x, \tilde{z}_+, \tilde{z})\| \times \\ & \qquad\qquad \times \|\tilde{g}(\tilde{\xi}, x, \Pi(\tilde{z} + z_\star(x)), \delta) + \Delta \xi_{\text{eq}}(x, \tilde{z}_+, \tilde{z})\| \\ & \quad + a_4 \|\Delta \xi_{\text{eq}}(x, \tilde{z}_+, \tilde{z})\| \left\| \tilde{g}(\tilde{\xi}, x, \Pi(\tilde{z} + z_\star(x)), \delta) \right\| \\ & \overset{(a)}{\leq} a_4 \|\Delta \xi_{\text{eq}}(x, \tilde{z}_+, \tilde{z})\|^2 \\ & \quad + 2 a_4 \|\Delta \xi_{\text{eq}}(x, \tilde{z}_+, \tilde{z})\| \left\| \tilde{g}(\tilde{\xi}, x, \Pi(\tilde{z} + z_\star(x)), \delta) \right\|, \end{aligned} \tag{45}$$

where (a) follows by the triangular inequality. By observing the definition of $\tilde{g}$ (cf. (18a)), we note that $\tilde{g}(0, x, \Pi(z_\star(x))) = 0$ for all $x \in \mathbf{X}$ in light of (2) (cf. Assumption 2). Thus, by combining this property with the Lipschitz continuity of $\tilde{g}$ (cf. Assumption 1), it holds

$$\left\| \tilde{g}(\tilde{\xi}, x, \Pi(\tilde{z} + z_\star(x)), \delta) \right\| \le L_g \left\| \tilde{\xi} \right\| + \| \tilde{z} \| . \tag{46}$$

By observing the definition of $\Delta \xi_{\mathrm{eq}}$ (cf. (18c)) and using the Lipschitz continuity of ξ_{eq} (cf. Assumption 2), we get

$$\begin{aligned} \| \Delta \xi_{\mathrm{eq}}(x, \tilde{z}_+, \tilde{z}) \| &\le L_\xi \| \Pi(\tilde{z}_+ + z_\star(x)) - \Pi(\tilde{z} + z_\star(x)) \| \\ &\overset{(a)}{\le} L_\xi \left\| \tilde{\mathcal{T}}(\tilde{z}, x) \right\| + L_\xi \| \tilde{z} \| \\ &\overset{(b)}{\le} L_\xi (L_\mathcal{T} + 1) \| \tilde{z} \| , \end{aligned} \tag{47}$$

where in (a) we use the Cauchy-Schwarz inequality, the fact that $\|\Pi\| = 1$, the definition of $\tilde{z}_+$ (cf. (43b)), and the triangle inequality, while in (b) we use the fact that $\tilde{\mathcal{T}}(0, x) = 0$ for all $x \in \mathbf{X}$ (see (13) in Assumption 3) and the Lipschitz continuity of $\tilde{\mathcal{T}}$ (cf. Assumption 3). Therefore, by using (46) and (47), we further bound the right-hand side of (45) as

$$U(\tilde{\xi}_+) - U(\tilde{\xi}_+^{\mathrm{nom}}) \le 2k_1 \left\| \tilde{\xi} \right\| \| \tilde{z} \| + k_2 \| \tilde{z} \|^2 , \tag{48}$$

in which we introduce the constants $k_1 := a_4 L_\xi L_g (L_\mathcal{T} + 1)$ and $k_2 := a_4 \left(2 L_\xi (L_\mathcal{T} + 1) + (L_\xi (L_\mathcal{T} + 1))^2 \right)$. In turn, by using (48), we bound the right-hand side of (44) as

$$\begin{aligned} \Delta \mathcal{U}(\tilde{\xi}, \tilde{z}) &\le -a_3 \left\| \tilde{\xi} \right\|^2 - (\kappa b_3 - k_2) \| \tilde{z} \|^2 + 2 k_1 \left\| \tilde{\xi} \right\| \| \tilde{z} \| \\ &\overset{(a)}{=} - \begin{bmatrix} \left\| \tilde{\xi} \right\| \\ \| \tilde{z} \| \end{bmatrix}^\top \underbrace{\begin{bmatrix} a_3 & -k_1 \\ -k_1 & \kappa b_3 - k_2 \end{bmatrix}}_{H(\kappa)} \begin{bmatrix} \left\| \tilde{\xi} \right\| \\ \| \tilde{z} \| \end{bmatrix} , \end{aligned} \tag{49}$$

where in (a) we adopt a compact matrix notation. By Sylvester criterion, we have

$$H(\kappa) \succ 0 \iff a_3(\kappa b_3 - k_2) > k_1^2 \iff \kappa > \frac{k_1^2}{a_3 b_3} + \frac{k_2}{b_3}.$$

The proof follows by accordingly setting κ and denoting with $d_3 > 0$ the smallest eigenvalue of $H(\kappa)$.

REFERENCES

[1] A. Bemporad, "Model predictive control design: New trends and tools," in *Proceedings of the 45th IEEE Conference on Decision and Control*. IEEE, 2006, pp. 6678–6683.
[2] B. Kouvaritakis and M. Cannon, "Model predictive control," *Switzerland: Springer International Publishing*, vol. 38, no. 13-56, p. 7, 2016.
[3] J. B. Rawlings, D. Q. Mayne, M. Diehl *et al.*, *Model predictive control: theory, computation, and design*. Nob Hill Publishing Madison, WI, 2020, vol. 2.
[4] U. Rosolia and A. D. Ames, "Multi-rate control design leveraging control barrier functions and model predictive control policies," *IEEE Control Systems Letters*, vol. 5, no. 3, pp. 1007–1012, 2020.
[5] N. Csomay-Shanklin, A. J. Taylor, U. Rosolia, and A. D. Ames, "Multi-rate planning and control of uncertain nonlinear systems: Model predictive control and control Lyapunov functions," in *2022 IEEE 61st Conference on Decision and Control (CDC)*. IEEE, 2022, pp. 3732–3739.
[6] U. Rosolia, A. Singletary, and A. D. Ames, "Unified multirate control: From low-level actuation to high-level planning," *IEEE Transactions on Automatic Control*, vol. 67, no. 12, pp. 6627–6640, 2022.
[7] N. Matni, A. D. Ames, and J. C. Doyle, "Towards a theory of control architecture: A quantitative framework for layered multi-rate control," *arXiv preprint arXiv:2401.15185*, 2024.
[8] M. Loehning, M. Reble, J. Hasenauer, S. Yu, and F. Allgoewer, "Model predictive control using reduced order models: Guaranteed stability for constrained linear systems," *Journal of Process Control*, vol. 24, no. 11, pp. 1647–1659, 2014.
[9] J. Lorenzetti, B. Landry, S. Singh, and M. Pavone, "Reduced order model predictive control for setpoint tracking," in *2019 18th European Control Conference (ECC)*. IEEE, 2019, pp. 299–306.
[10] J. Lorenzetti and M. Pavone, "Error bounds for reduced order model predictive control," in *2020 59th IEEE Conference on Decision and Control (CDC)*. IEEE, 2020, pp. 2521–2528.
[11] M. Kartmann, M. Manucci, B. Unger, and S. Volkwein, "Certified model predictive control for switched evolution equations using model order reduction," *arXiv preprint arXiv:2412.12930*, 2024.
[12] W. Wang and J. P. Koeln, "Tube-based robust MPC for two-timescale systems using reduced-order models," *IEEE Control Systems Letters*, vol. 7, pp. 799–804, 2022.
[13] M. Diehl, H. G. Bock, and J. P. Schlöder, "A real-time iteration scheme for nonlinear optimization in optimal feedback control," *SIAM Journal on control and optimization*, vol. 43, no. 5, pp. 1714–1736, 2005.
[14] S. Gros, M. Zanon, R. Quirynen, A. Bemporad, and M. Diehl, "From linear to nonlinear MPC: bridging the gap via the real-time iteration," *International Journal of Control*, vol. 93, no. 1, pp. 62–80, 2020.
[15] P. O. Scokaert, D. Q. Mayne, and J. B. Rawlings, "Suboptimal model predictive control (feasibility implies stability)," *IEEE Transactions on Automatic Control*, vol. 44, no. 3, pp. 648–654, 2002.
[16] K. Graichen and A. Kugi, "Stability and incremental improvement of suboptimal MPC without terminal constraints," *IEEE Transactions on Automatic Control*, vol. 55, no. 11, pp. 2576–2580, 2010.

[17] M. Rubagotti, P. Patrinos, and A. Bemporad, "Stabilizing linear model predictive control under inexact numerical optimization," *IEEE Trans. on Automatic Control*, vol. 59, no. 6, pp. 1660–1666, 2014.

[18] A. Karapetyan, E. C. Balta, A. Iannelli, and J. Lygeros, "On the finite-time behavior of suboptimal linear model predictive control," in *2023 62nd IEEE Conference on Decision and Control (CDC)*. IEEE, 2023, pp. 5053–5058.

[19] ——, "Closed-loop finite-time analysis of suboptimal online control," *IEEE Transactions on Automatic Control*, 2025.

[20] A. Zanelli, Q. Tran-Dinh, and M. Diehl, "A Lyapunov function for the combined system-optimizer dynamics in inexact model predictive control," *Automatica*, vol. 134, p. 109901, 2021.

[21] Y. Chen, F. Bullo, and E. Dall'Anese, "Sampled-data systems: Stability, contractivity and single-iteration suboptimal MPC," *arXiv preprint arXiv:2505.18336*, 2025.

[22] G. Carnevale, F. Fabiani, F. Fele, K. Margellos, and G. Notarstefano, "Tracking-based distributed equilibrium seeking for aggregative games," *IEEE Transactions on Automatic Control*, pp. 1–16, 2024.

[23] V. Chellaboina and W. M. Haddad, *Nonlinear dynamical systems and control: A Lyapunov-based approach*. Princeton University Press, 2008.